Supporting Information

A quantitative identification fluorescence probe for highly selective detection of Cu^{2+} in food and environmental samples

Hui Xu [a], Jianing Zhang [a], Xiaomei Ren [a], Yating Zhang [a], Yuanlan Yang [a], Xinyi Zhou [a], Wenjian Yang [a], Minhao Xie [a], Jiawei Yang [b], Xin Wang [b], Zhenwei Yuan* [b], Ji Liu* [b]*

AUTHOR ADDRESS

[a] *Collaborative Innovation Center for Modern Grain Circulation and Safety, Jiangsu Province Engineering Research Center of Edible Fungus Preservation and Intensive Processing, College of Food Science and Engineering, Nanjing University of Finance and Economics, Nanjing 210023, China.*

[b] *Department of Biomedical Engineering, School of Engineering, China Pharmaceutical University, 639 Longmian Road, Jiangning, Nanjing, 210009 China.*

** For correspondence: Hui Xu, e-mail:9120191156@nufe.edu.cn; Zhenwei Yuan, e-mail: yuanzhenwei@cpu.edu.cn; Ji Liu, e-mail: jiliu1618@163.com.*

2.1 Experimental section

2.1.1Reagents and instrumentation

All chemical reagents and solvents were stemmed from commercial suppliers and were used directly unless otherwise specified. The Human cervical cancer (Hela) cell lines were purchased from the cell bank of Shanghai academy of life sciences, Chinese academy of sciences (Shanghai, China). Trypsin (2500 U/mg), Minimum Essential Medium (MEM), and penicillin-streptomycin were purchased from Hyclone (Utah, America). Fetal bovine serum (FBS) was purchased from Gibco (New York, America).

^{1}H NMR and ^{13}C NMR spectra were measured with AV400 NMR instruments, which were purchased from Bruker (Massachusetts, America). 15 mg of sample was weighed and dissolved in 0.6 mL of deuterated chloroform for NMR spectroscopic analysis. All NMR spectra were acquired on a 400 MHz spectrometer, and the number of scans were 1024 for both ^{1}H NMR and ^{13}C NMR. Chemical changes were reported in units of one part per million (ppm). High-resolution mass spectrometry (HR-MS) characterization was conducted on a Waters G2-XS Q-TOF instrument (Massachusetts, America) with an m/z detection range of 50 to 1200 m/z. Analytical samples RC-1 and RC-2 (2 mg each) were dissolved in acetonitrile for molecular mass and structural elucidation. UV-Vis absorption spectra were measured using the UV-2550 fluorescence spectrophotometer purchased from Shimadzu (Kyoto, Japan), while the emission spectrum was recorded on a Hitachi F-7000 spectrofluorometer (Tokyo, Japan). The fluorescence images were collected by LSM900, which was purchased from Zeiss (Oberkochen, Germany). The pH was measured with a PHS-3C pH meter from Leici (Shanghai, China).

2.1.2 Synthesis of compound ZR

The reaction was carried out by dissolving (4-(diphenylamino) phenyl) boronic acid (1) (1.735 g, 6 mmol), 4-bromo-2-hydroxybenzaldehyde (2) (1.447 g, 7.2 mmol), anhydrous K_2CO_3 (4.14 g, 30 mmol), and $PdCl_2$ (dppf) catalyst (0.439 g, 0.6 mmol) in a toluene/ethanol (v/v 2:1) solvent mixture. The reaction mixture was maintained under nitrogen protection at 60°C for 5 h. After cooling to room temperature, the solvent was removed via vacuum distillation, and the crude product was purified by column chromatography using an EA/PE (v/v, 1:10) solvent system to afford compound ZR (1.91 g, 87.17%). ^{1}H NMR (400 MHz, Chloroform-*d*) δ 11.12 (s, 1H), 9.87 (s, 1H),

7.56 (d, J = 8.1 Hz, 1H), 7.50 (d, J = 8.7 Hz, 2H), 7.32-7.26 (m, 4H), 7.25-7.20 (m, 1H), 7.19-7.11 (m, 6H), 7.08 (dd, J = 13.5, 6.3 Hz, 3H); ^{3}C NMR (101 MHz, Chloroform-d) δ 195.87, 162.16, 149.38, 148.95, 147.37, 134.20, 132.27, 129.57, 128.19, 125.16, 123.75, 122.87, 119.31, 118.32, 114.90. LCMS: (ESI, *m/z*) Calcd for $C_{25}H_{19}NO_2$ [M+H]: 366.14, found 366.15.

2.1.3 Preparation of solutions of probes and analytes

Stock solutions of probes RC-1 and RC-2 were prepared in tetrahydrofuran (THF) at a concentration of 10.0 mM, and subsequently diluted to 1.0 mM working concentrations. Stock solutions of the analytes (Cu^{2+}, Na^{+}, Zn^{2+}, Ag^{+}, K^{+}, Ca^{2+}, Mn^{2+}, Hg^{2+}, Fe^{2+}, Mg^{2+}, Fe^{3+}, Co^{2+}, Cr^{3+}, Ni^{2+}, Ba^{2+}, Br^{-}, F^{-}, HSO_3^{-}, Cl^{-}, NO_3^{-}, SO_4^{2-} and CO_3^{2-}) were prepared at the concentration of 4.0 mM using deionized water. The process was monitored by fluorescence spectrometer (λ_{ex} = 385 nm/λ_{ex} = 396 nm, slit:5 nm/10 nm).

2.1.4 Preparation and determination of real samples

The food samples used in this study included orange juice, mineral water and rock sugar were obtained from a local supermarket, the tap water was sourced from Nanjing University of Finance and Economics (Nanjing China). Lake water was used as environmental sample (Nanjing, China). All samples were acquired following compliance with local regulations and stored at 4°C prior to analysis. Solid rock sugar samples were homogenized by mechanical cutting, and a 0.5 g sample was digested with 5 mL of HNO_3 using microwave-assisted acid digestion., The digestates were quantitatively transferred and diluted to 50 mL with ultrapure water. Liquid samples (1.0 mL) underwent identical digestion (5 mL HNO_3) and dilution protocols.

2.1.5 ICP-MS experiments

The preparation method of the sample is the same as 2.1.4. Dilute the standard curve sample with 5% HNO_3, prepare the standard solution and use it immediately. Comparative analysis of real samples was recorded on an Agilent 7700x Inductively Coupled Plasma Mass Spectrometer (California America).

2.1.6 Development of a mini program for smartphone

To facilitate the calculation of Cu^{2+} content, a WeChat Mini Program was successfully developed. The design of this mini program involved inputting the fluorescence value obtained from the fluorescence spectrometer, along with the corresponding blank value, into designated input fields. The Cu^{2+} concentration (x) was determined using the following equation based on the detection limit of probe RC-2:

$$y-b = -1198.2\ x+1943.3$$

where:

b = intrinsic fluorescence of the sample (blank value)

y = fluorescence intensity of the sample+probe (test value)

The calculated x value was then converted to the total copper content. Notably, the mini-program operates only needs to input the values of samples to run, and does not require standard curve equations or fluorescence values. Finally, the obtained results were compared with the established safety thresholds and the safety of the food was evaluated for consumption.

2.1.7 Cell imaging and cytotoxicity determination

HeLa cells were cultured at 37℃ in 5% CO_2 atmosphere using MEM supplemented 10% fetal bovine serum (FBS) and 1% antibiotics solution (containing 100 U/mL penicillin and 100 μg/mL streptomycin). Prior to fluorescence imaging, the cytotoxic effect of probe RC-2 was evaluated through thiazolyl blue tetrazolium bromide (MTT) viability assay. For imaging experiments, one cell group served as the blank group, while the test group was incubated with probe RC-2 (10 μM) for 1 hour at 37℃ prior to microscopic analysis. In the experimental group, cells were initially treated with probe RC-2 (10 μM) for 1 hour at 37℃. Following removal of the probe-containing medium, the cells were subsequently exposed to Cu^{2+} (10 μM) for an additional 30 minutes incubation prior to fluorescence imaging. Before imaging, the culture media was removed and cells were washed three times with phosphate buffer solution (PBS, pH = 7.4). Cellular imaging was then performed using an LSM900 laser scanning confocal microscope.

2.1.8 In situ determination of Cu^{2+} in plant tissues

Baby cabbage seeds were first germinated under controlled humidity conditions at 20℃ for 12 hours. Subsequently, the germinated seeds were transferred to sterile

moistened gauze and maintained under identical temperature conditions for an additional 48 hours of incubation. Following a total incubation period of 60 hours, seedling root tips were harvested for analysis. Untreated samples served as the blank group and were immediately subjected to imaging. After incubating the control group root tips with the probe RC-2 (10 μM) for 1 hour, imaging was performed. In the experimental group, the root tips were first incubated with the probe for 1 hour. Following the removal of the probe solution, the root tips were treated with a 10 μM Cu^{2+} solution for 30 minutes before imaged.

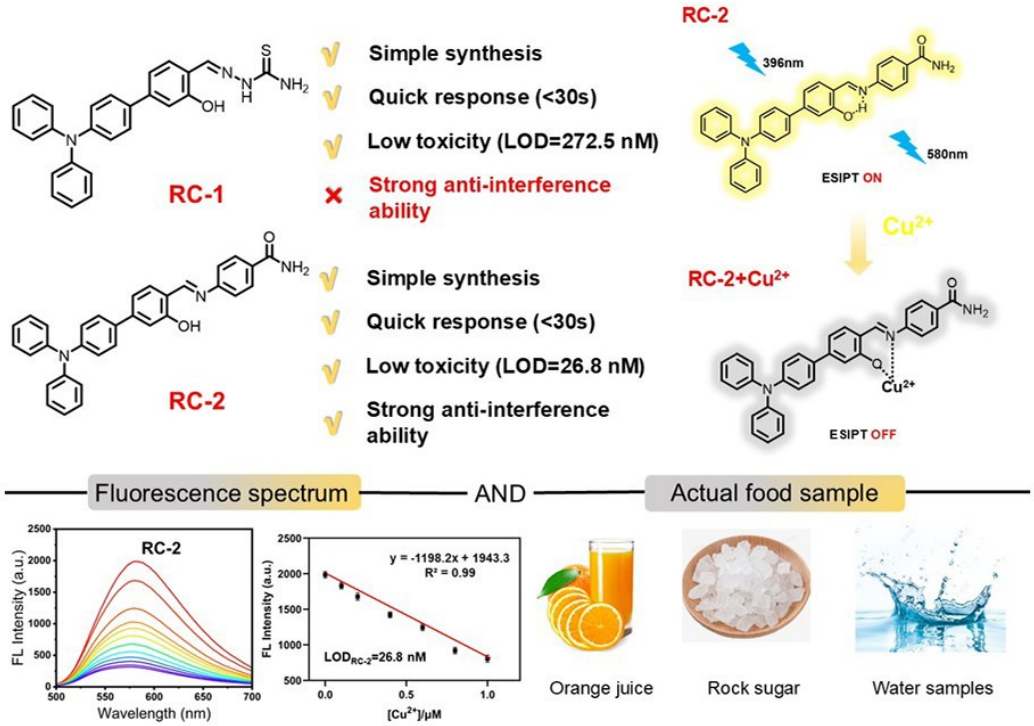

Figure S1. The interaction mechanism of compound RC-2 with Cu^{2+}.

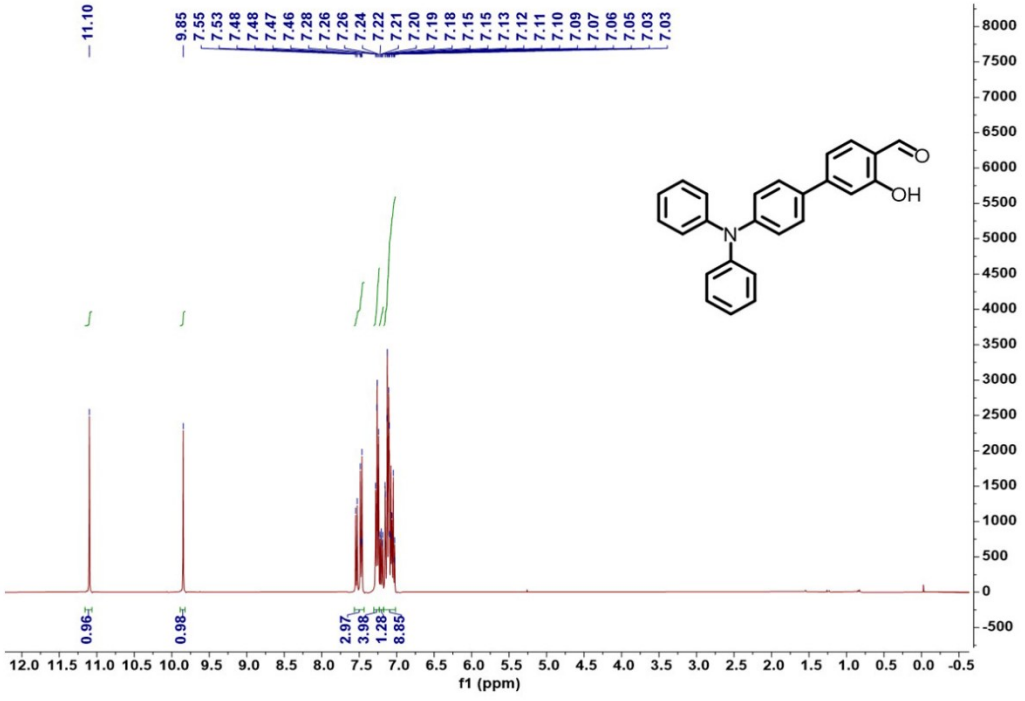

Figure S2. ^{1}H NMR spectrum of ZR in Chloroform-*d*.

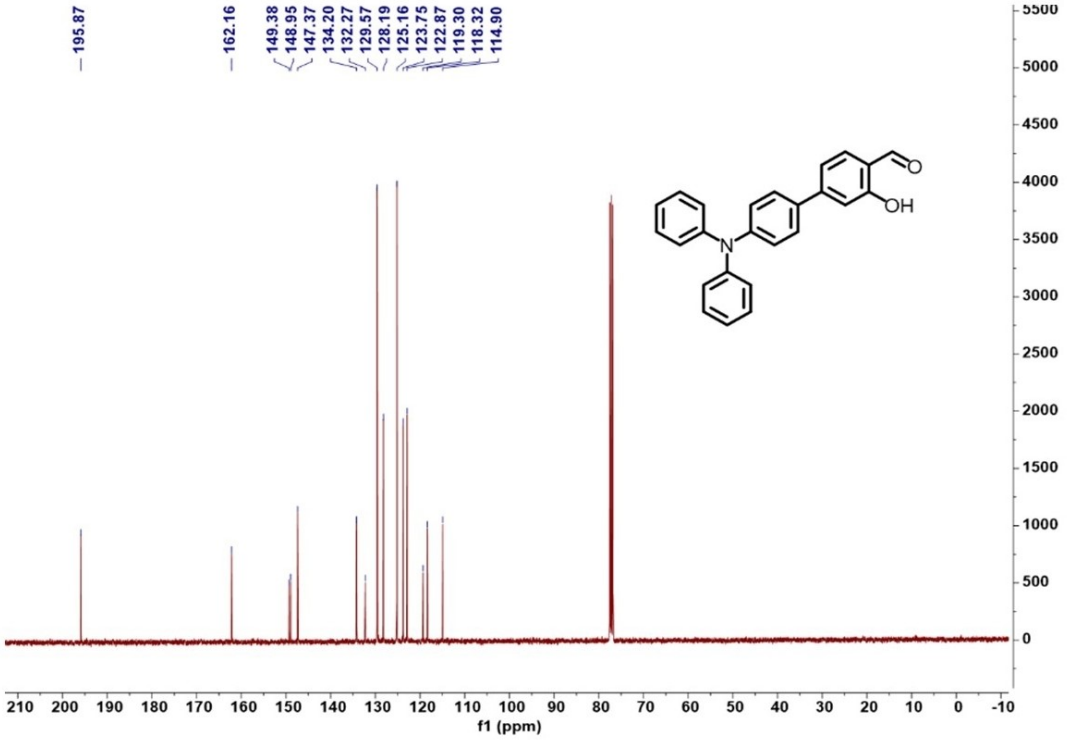

Figure S3. ^{13}C NMR spectrum of ZR in Chloroform-*d*.

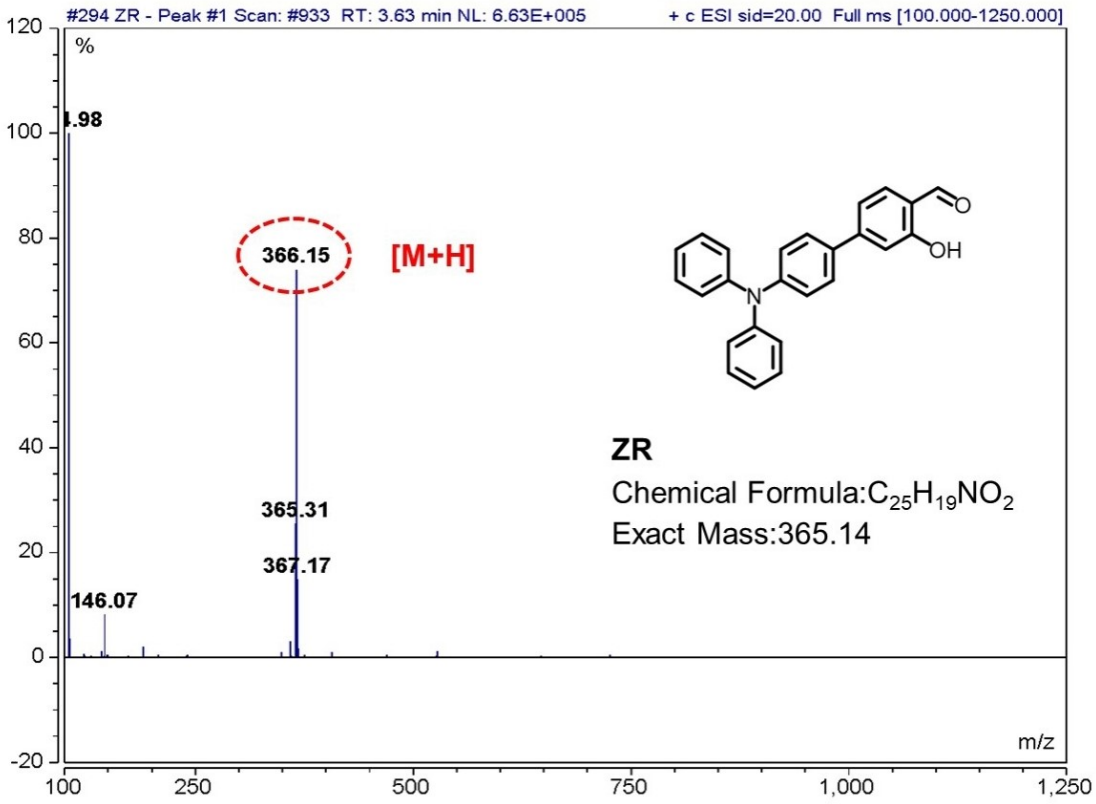

Figure S4. LC-MS spectrum of ZR.

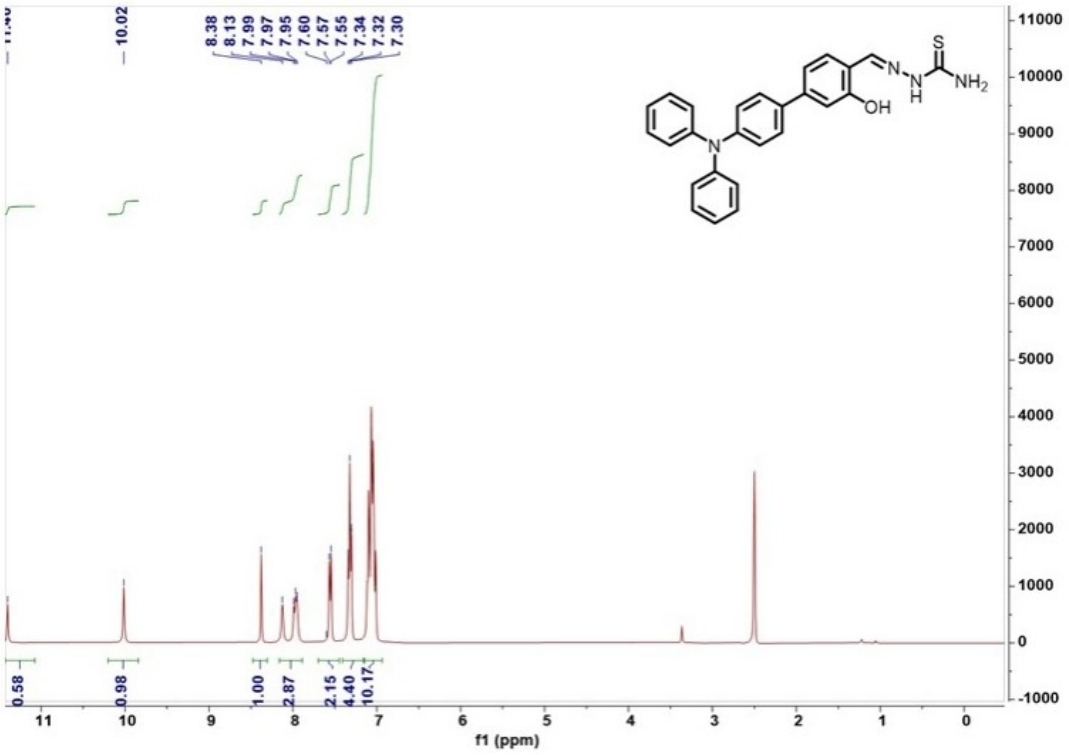

Figure S5. ^{1}H NMR spectrum of probe RC-1 in Chloroform-*d*.

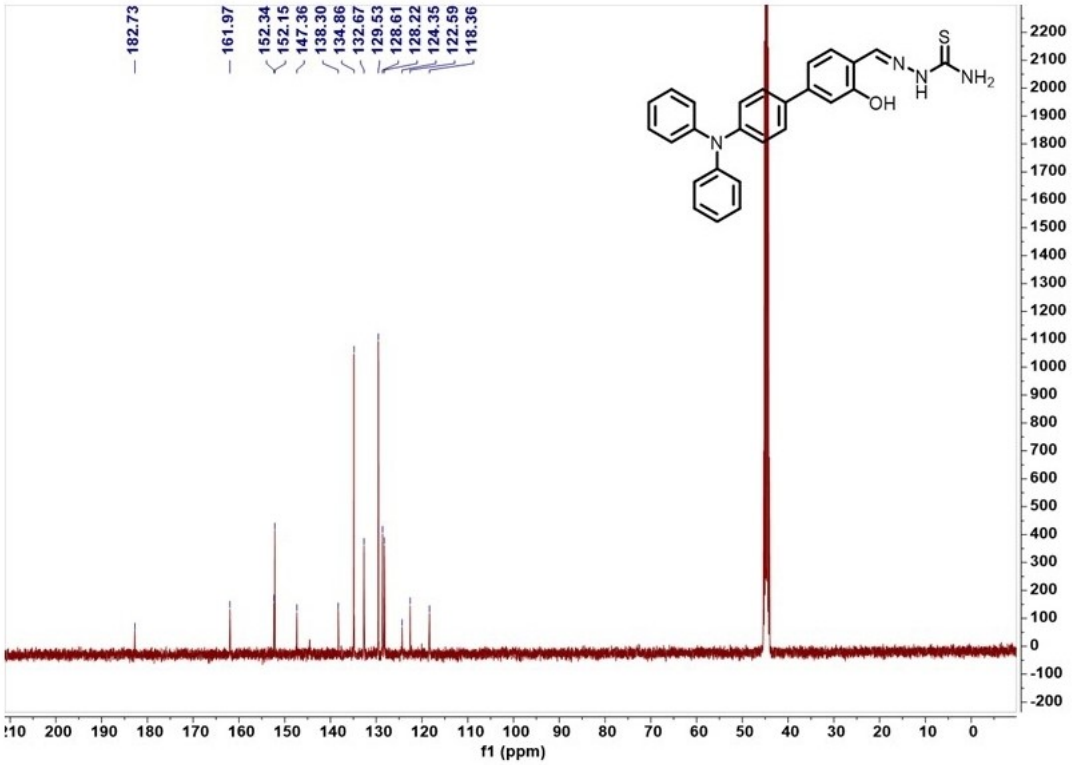

Figure S6. ^{13}C NMR spectrum of probe RC-1 in Chloroform-*d*.

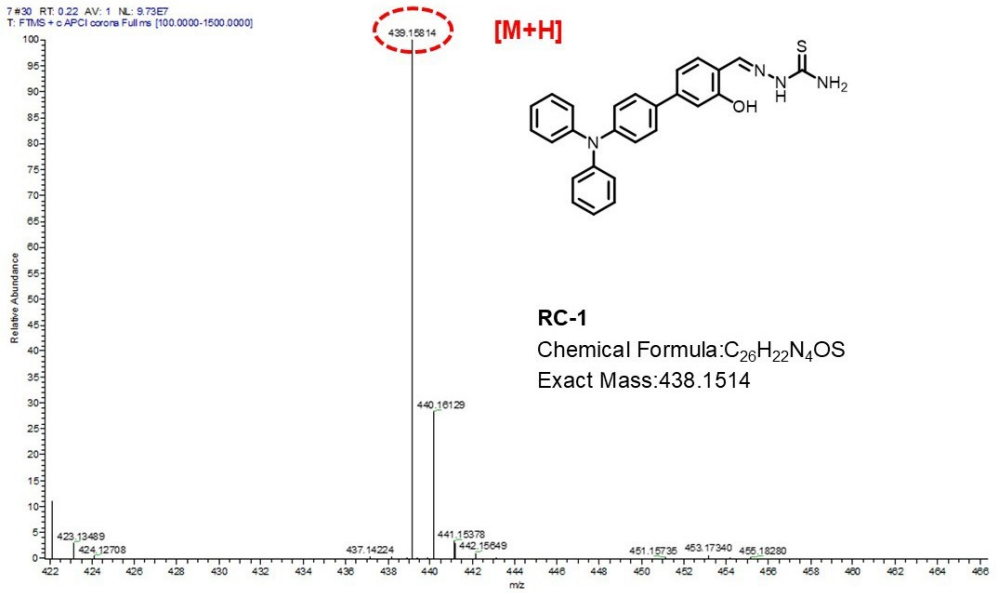

Figure S7. HR-MS spectrum of probe RC-1.

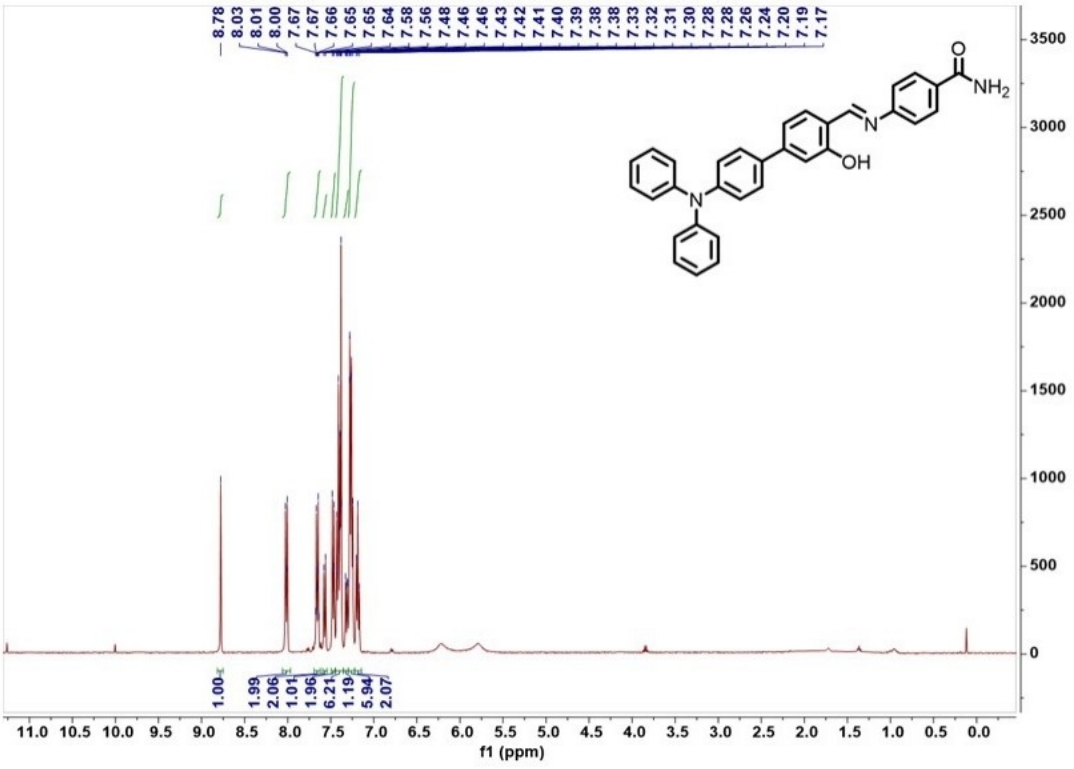

Figure S8. ^{1}H NMR spectrum of probe RC-2 in Chloroform-*d*.

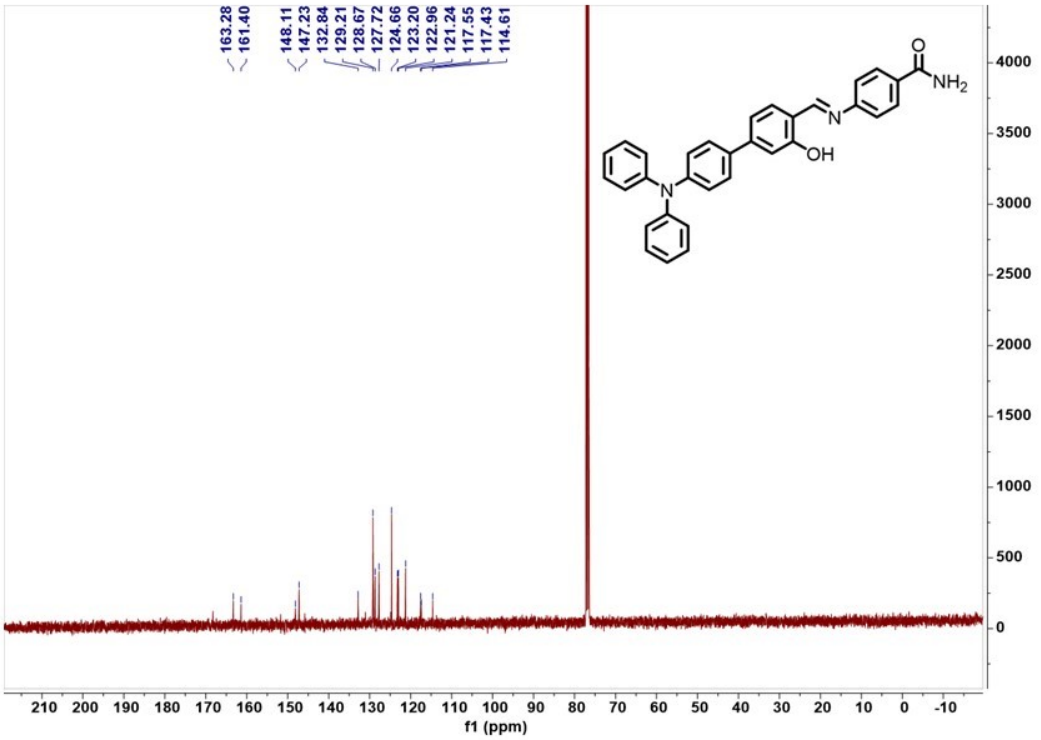

Figure S9. ^{13}C NMR spectrum of probe RC-2 in Chloroform-*d*.

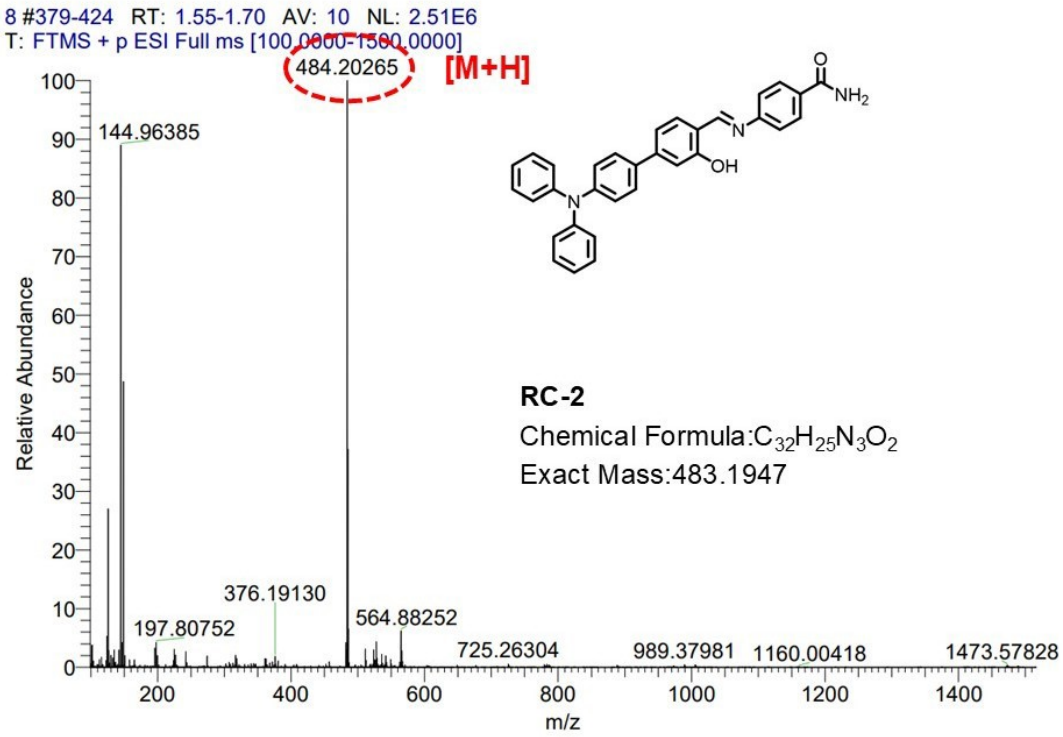

Figure S10. HR-MS spectrum of probe RC-2.

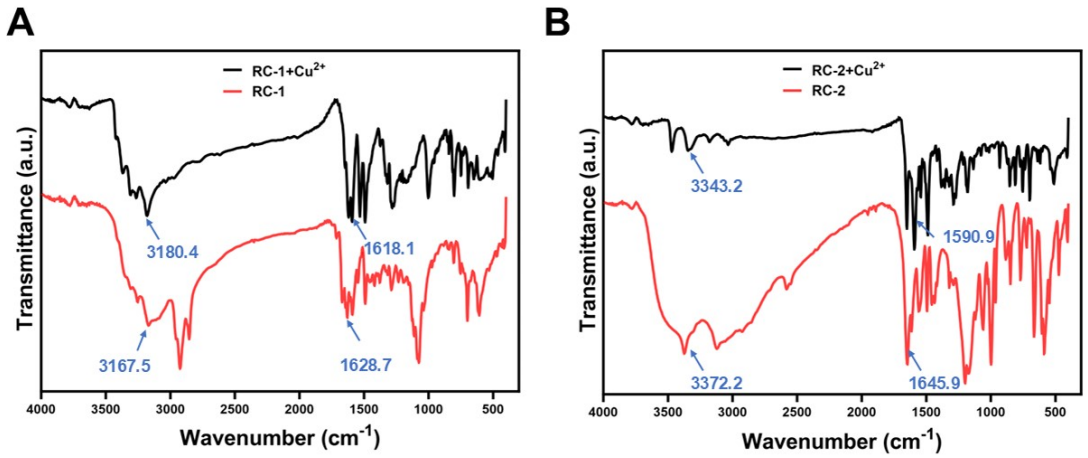

Figure S11. FTIR spectra of RC-1 and RC-2 probes, as well as their complexes with Cu^{2+}.

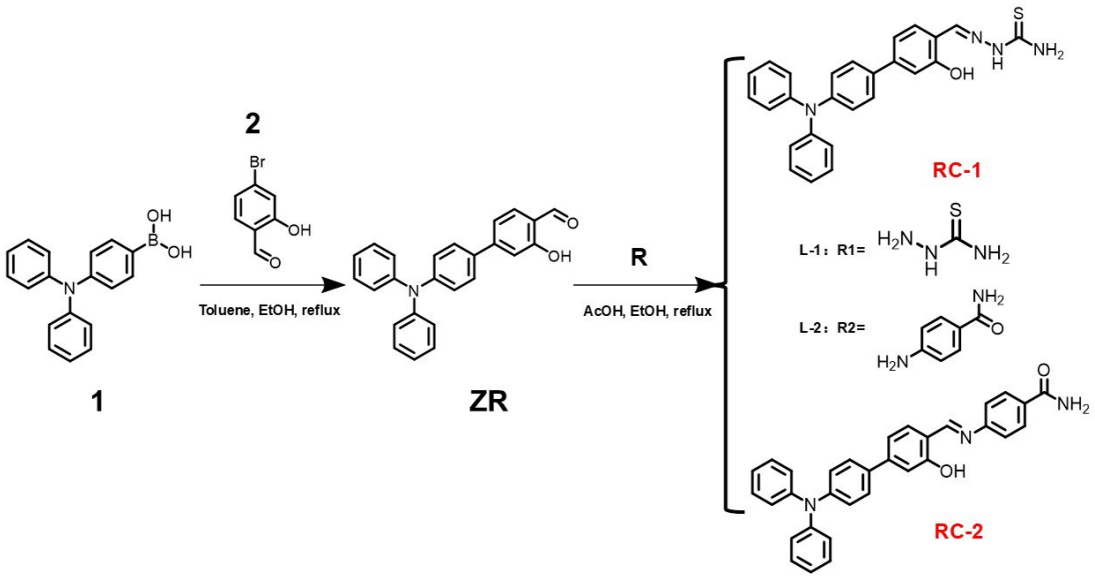

Figure S12. The synthesis strategy of compounds RC-1 and RC-2.

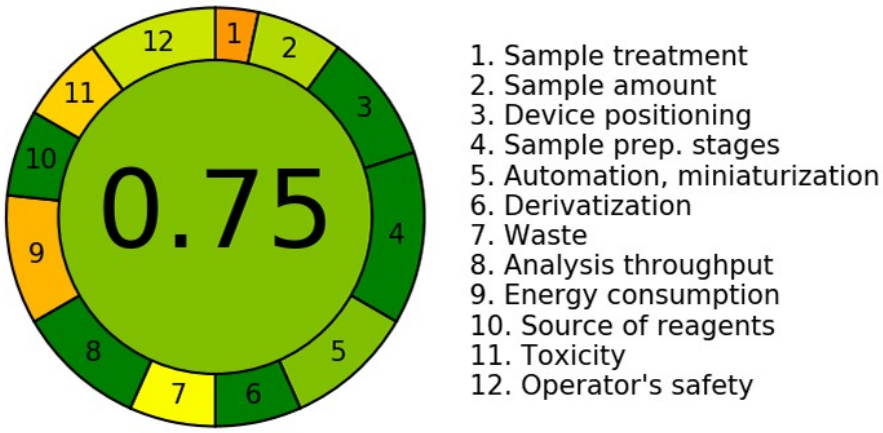

Figure S13. Green index evaluation of probe RC-2

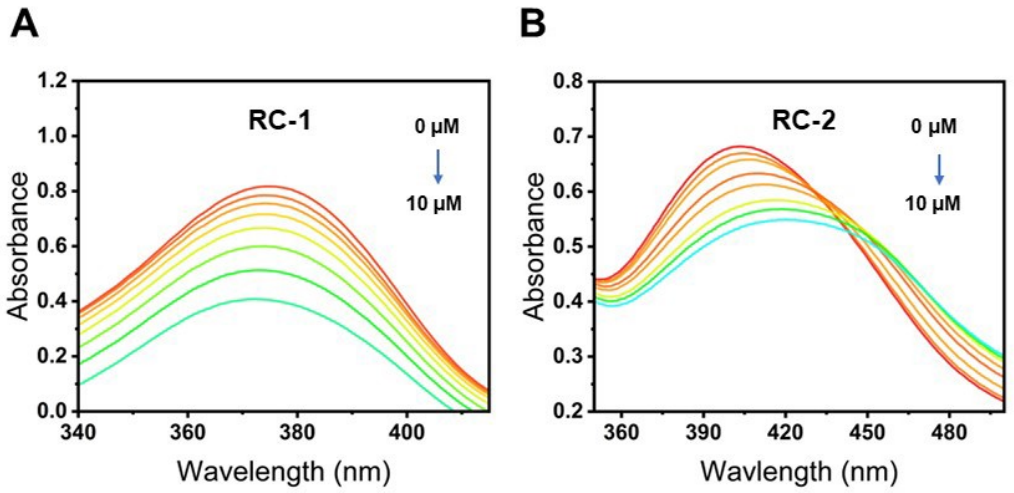

Figure S14. (A) UV absorption spectra change of probe RC-1 (10 μM) reacting with Cu^{2+} (0-10 μM). (B) UV absorption spectra change of probe RC-2 (10 μM) reacting with Cu^{2+} (0-10 μM).

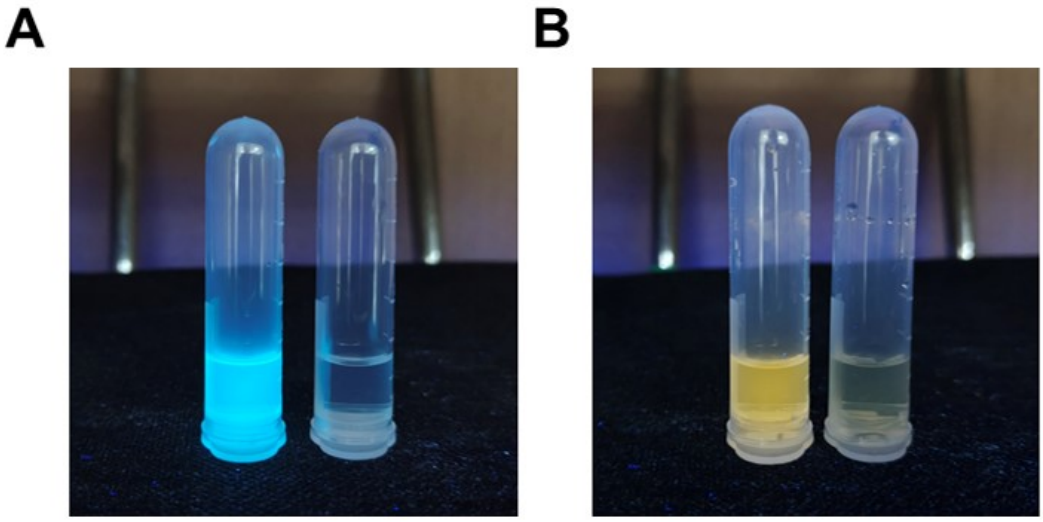

Figure S15. The photographs of fluorescent RC-1 and RC-2 probes with and without Cu^{2+} analyte.

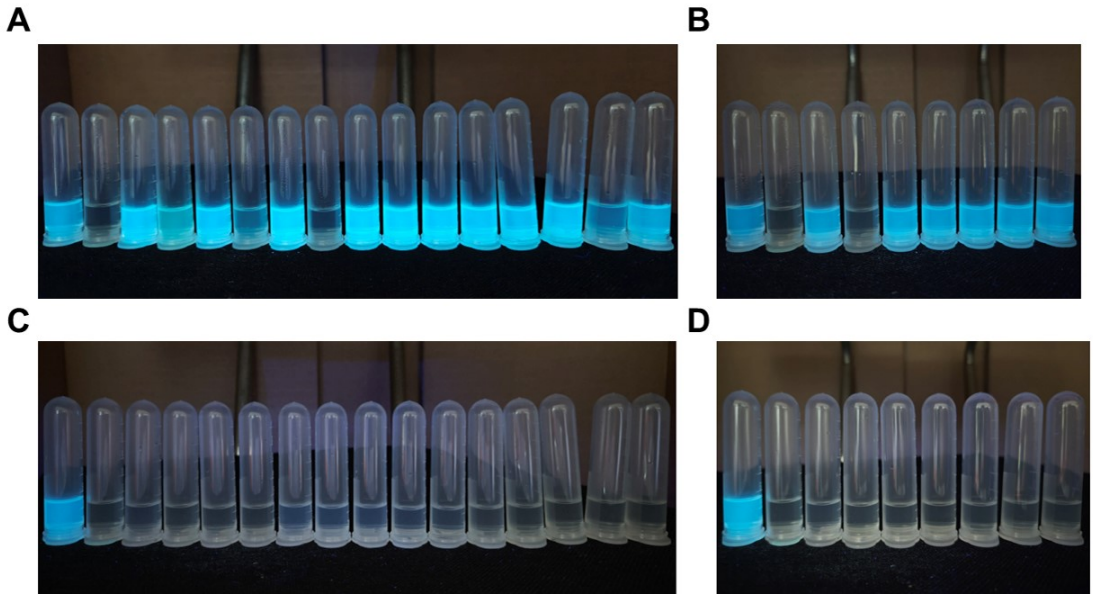

Figure S16. Comparison of images of probe RC-1 before and after adding Cu^{2+} under ultraviolet light after adding cation (A) and anion (B) ions. From left to right is (A) the blank group, Cu^{2+}, Na^{+}, Zn^{2+}, Fe^{2+}, Hg^{2+}, Ag^{+}, Co^{2+}, Ca^{2+}, Mn^{2+}, K^{+}, Mg^{2+}, Fe^{3+}, Ba^{2+}, Ni^{2+}, and Cr^{3+}. (B) the blank group, Cu^{2+}, Br^{-}, F^{-}, HSO_3^{-}, Cl^{-}, NO_3^{-}, SO_4^{2-}, and CO_3^{2-}. After adding copper ions, cations (C) and anions (D) competitively select images under ultraviolet light.

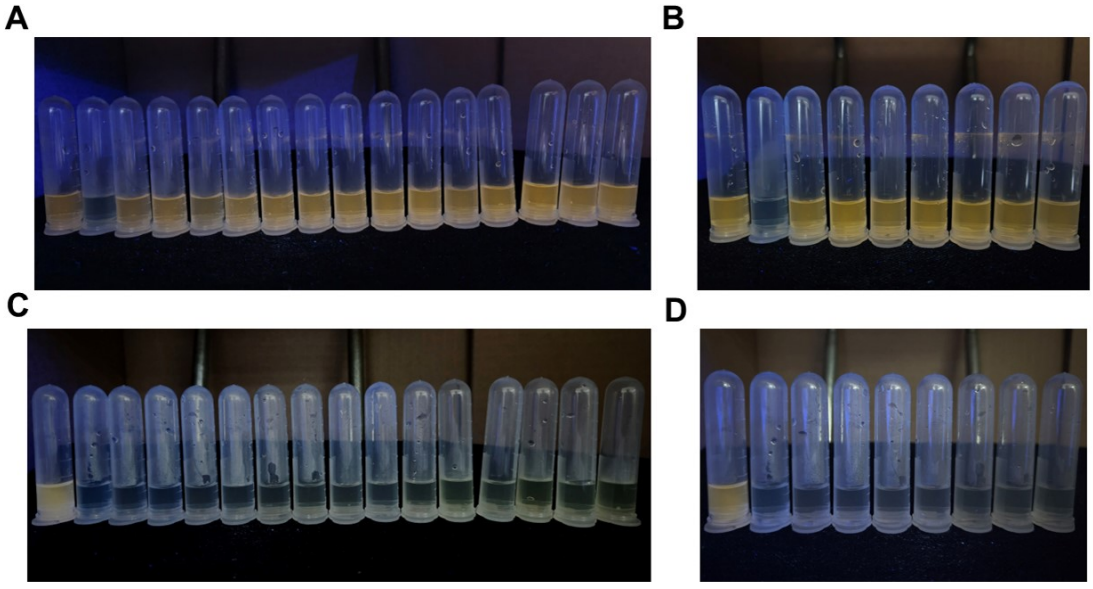

Figure S17. Comparison of images of probe RC-2 before and after adding Cu^{2+} under ultraviolet light after adding cation (A) and anion (B) ions. From left to right is (A) the blank group, Cu^{2+}, Na^{+}, Zn^{2+}, Fe^{2+}, Hg^{2+}, Ag^{+}, Co^{2+}, Ca^{2+}, Mn^{2+}, K^{+}, Mg^{2+}, Fe^{3+}, Ba^{2+},

Ni^{2+}, and Cr^{3+}. (B) the blank group, Cu^{2+}, Br^{-}, F^{-}, HSO_3^{-}, Cl^{-}, NO_3^{-}, SO_4^{2-}, and CO_3^{2-}. After adding copper ions, cations (C) and anions (D) competitively select images under ultraviolet light.

Table S1. The interference level of each interference source in the anti-interference experiment of RC-2.

Interferent	Concentration(μM)	Interference Level of RC-2 (%)
Na^{+}	10	0.27±0.04
Zn^{+}	10	-0.45±0.04
Fe^{2+}	10	-0.52±0.03
Hg^{2+}	10	-0.14±0.01
Ag^{+}	10	0.10±0.04
Co^{2+}	10	0.33±0.03
Ca^{2+}	10	1.63±0.02
Mn^{2+}	10	-0.19±0.03
K^{+}	10	0.69±0.03
Mg^{2+}	10	-0.31±0.04
Fe^{3+}	10	-0.20±0.01
Ba^{2+}	10	1.03±0.04
Ni^{2+}	10	0.56±0.02
Cr^{3+}	10	3.30±0.03
Br^{-}	10	0.42±0.04
F^{-}	10	-1.53±0.04
HSO_3^{-}	10	0.33±0.03
Cl^{-}	10	-1.53±0.02
NO_3^{2-}	10	-0.15±0.02
SO_4^{2-}	10	0.25±0.05
CO_3^{2-}	10	0.27±0.02

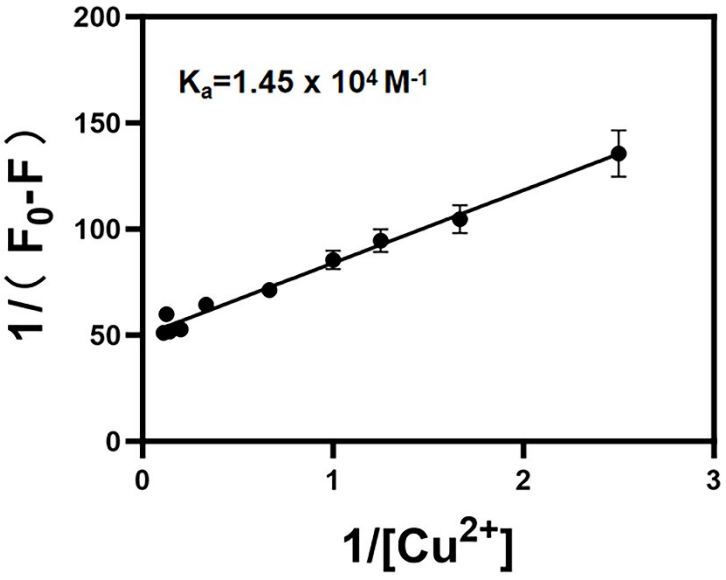

Figure S18. Benesi-Hildebrand plot of RC-2

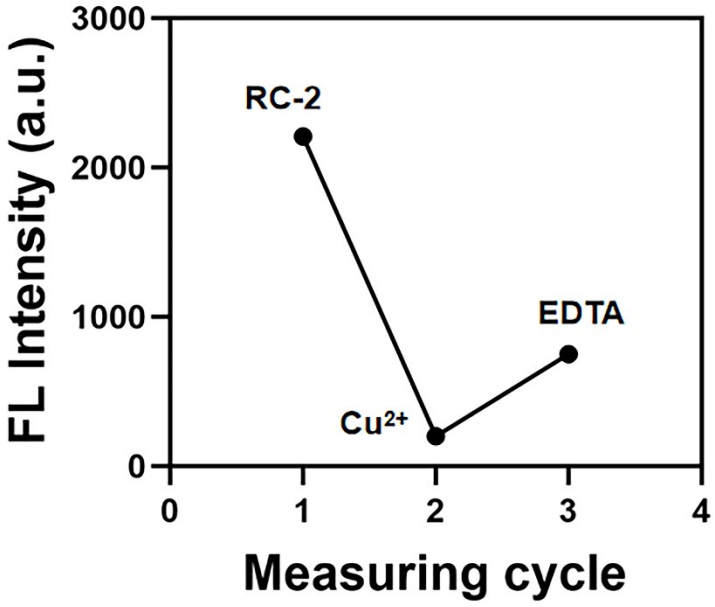

Figure S19. Reusability experiment of probe RC-2

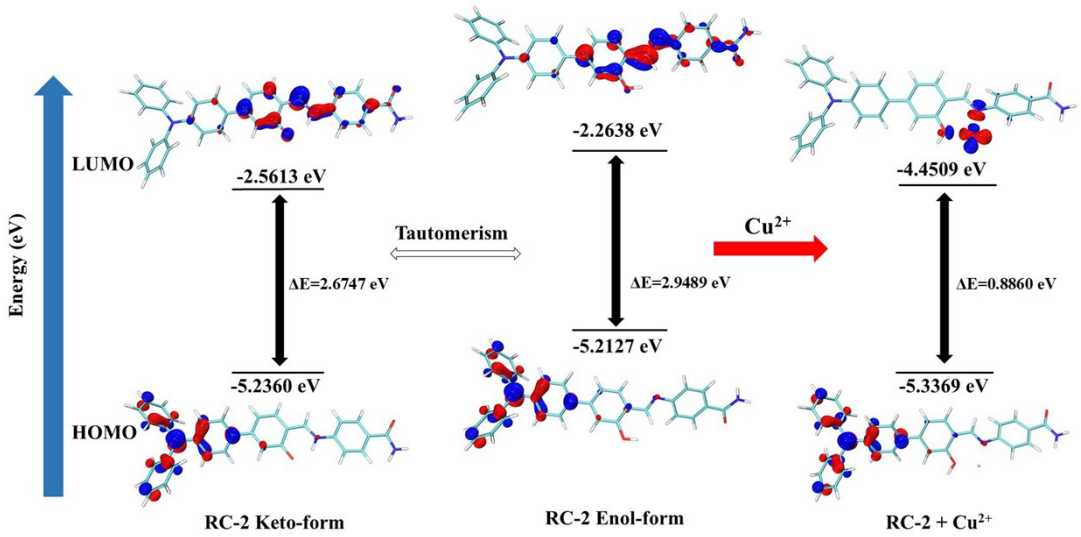

Figure S20. Computationally derived HOMO-LUMO energy levels for RC-2 and its Cu^{2+} complex.

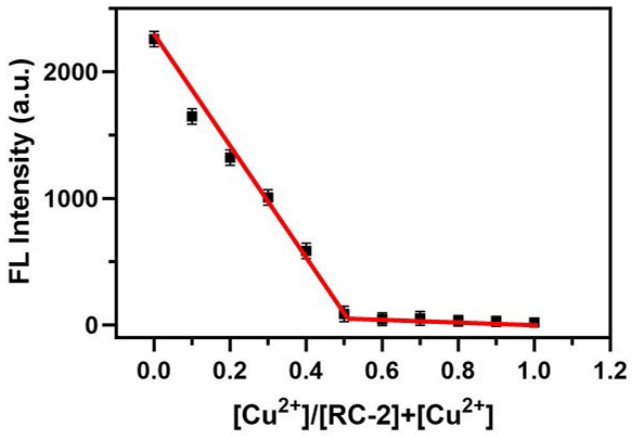

Figure S21. Job's plot for determining the stoichiometry of RC-2 and Cu^{2+} in a solvent mixture of THF/H_2O (at a 1:9 vol ratio).

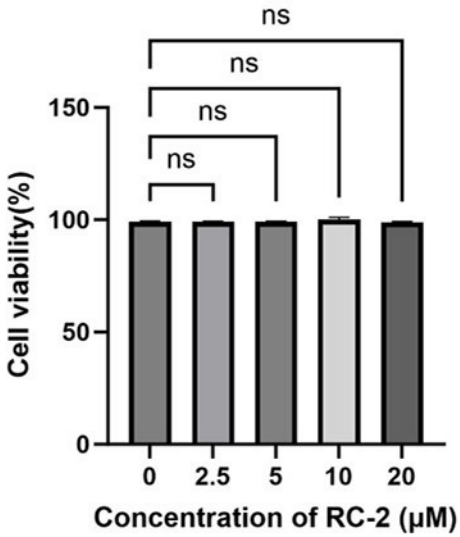

Figure S22. The viability of Hela cells incubated with probe RC-2 (0-20 μM) for 12 h.

Comparison of the performance of organic small molecule fluorescent probes for detecting copper ions

Table S2. Organic small molecule fluorescent probe for copper ion detection.

Name	Chemical structure	Synthesis route and technique	Detection limits (μM)	Linear range (μM)	Response time	pH	Application	Key Advantages	Key Limitations	Reference
OAHP	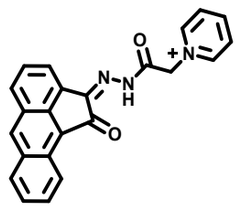	One-step synthesis	0.018	0.05~2	30 min	\	imaging and water	sensitive response and simple synthesis	long response time	[1]
PEG-R	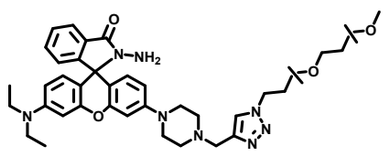	Four-step synthesis	1.295	0~125	15 min	4.5~10.5	imaging and food	wide pH range	complex synthesis and long response time	[2]
QLP	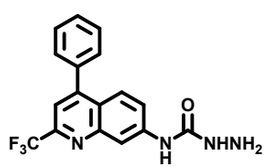	Two-step synthesis	0.087	0~10	2 min	4~10	food, environment and imaging	wide pH range and sensitive response	long response time	[3]

4	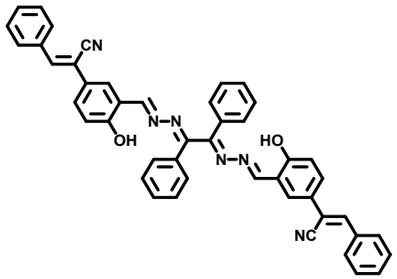	Two-step synthesis using Schiff base and knoevenagel condensation respectively	0.016	0~10	\	7.4	water and test paper	sensitive response	narrow pH range	4
1	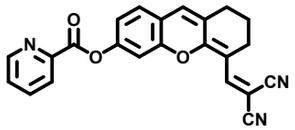	Five-step synthesis using condensation	0.004	0.02~8	40 min	7.4	food, plant tissue and zebrafish	sensitive response	narrow pH range long response time	5
A5	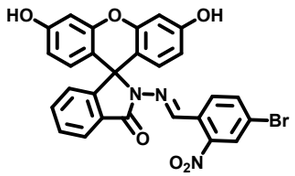	Two-step synthesis	0.11	10~40	2 min	6~9	test paper and cell imaging	wide pH range and sensitive response	long response time	6
R1	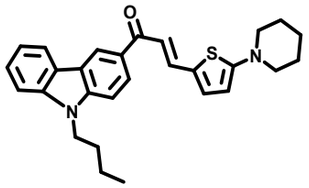	Four-step synthesis using aldol condensation	0.29	1~90	\	8~12	cell imaging	wide pH range and sensitive response	complex synthesis	7

3	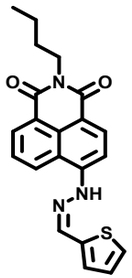	Three-step synthesis using Schiff base condensation	0.009	0~25	3 min	2~7	cell and water	sensitive response	pH is slightly acidic and synthesis is complex	[8]
NC-Cu	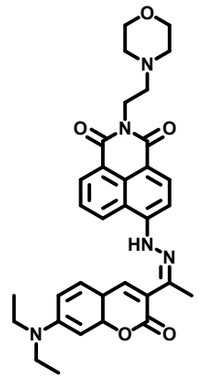	Four-step synthesis	5.8×10^{3}	0~1.2×10^{5}	20 min	7.4	cell imaging	high portability	high cost, low sensitivity	[9]
DHUCu-1	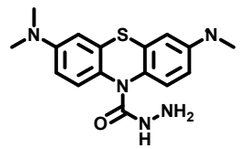	Two-step synthesis	0.019	0~3	\	7.2	cell imaging	sensitive response	narrow pH range	[10]
L	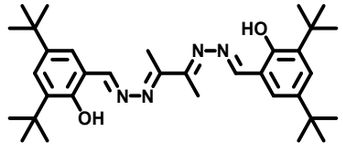	Two-step synthesis	0.53	0~4	15 min	4~13	water and test paper	wide pH range	long response time	[11]

GT-TSC	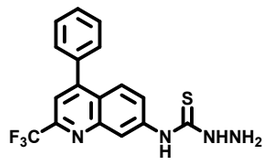	There-step synthesis	0.065	0.1-10	5 min	6~7.5	environment, food, cell and zebrafish imaging	sensitive response	narrow pH range	[12]
PN	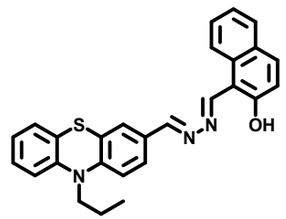	Four-step synthesis	0.179	0~10	1 min	6~13	water and test paper	short response time	complex synthesis	[13]
This work	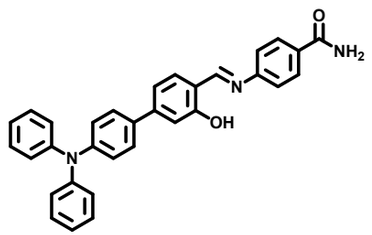	One-step synthesis	0.027	0~1	30 s	3~13	food, plant root tip and cell imaging, mini programs	short response time, simple synthesis	relies on a spectrofluorometer	

Reference

1. K. N. Okamoto Y, Hagimori M, et al, *Anal. Chim. Acta*, 2022, **1217**, 340024.
2. X. Q. Sun H, Xu C, et al, *Food Chem.*, 2023, **418**, 135994.
3. L. M. Zhu H, Liu C, et al, *Science of The Total Environment,*, 2023, **857**, 159488.
4. Z. M. Zhu M, Chen M, et al, *Opt. Mater.*, 2022, **125**, 112059.
5. Z. Zhou, H. Tang, S. Chen, Y. Huang, X. Zhu, H. Li, Y. Zhang and S. Yao, *Food Chem.*, 2021, **343**, 128513.
6. X. Leng, D. Wang, Z. Mi, Y. Zhang, B. Yang and F. Chen, *Biosensors*, 2022, **12**, 732.
7. W. P. Wang H, Niu L, et al, *Spectrochim. Acta, Part A*, 2022, **278**, 121257.
8. Y. L. Liu Y L, Li P, et al, *Spectrochim. Acta, Part A*, 2020, **227**, 117540.
9. Z. W. Ahmed N, Zhang D, et al., *Spectrochimica Acta Part A: Molecular and Biomolecular Spectroscopy,*, 2022, **264**, 120313.
10. Y. Chen, Z. Long, C. Wang, J. Zhu, S. Wang, Y. Liu, P. Wei and T. Yi, *Dyes Pigm.*, 2022, **204**, 110472.
11. M. Sahu, A. Manna and G. Patra, *Inorg. Chim. Acta*, 2020, **517**, 120199.
12. M. Liu, H. Zhu, K. Wang, X. Zhang, X. Li, M. Yu, B. Zhu, W. Sheng and C. Liu, *ACS Food Sci. Technol.*, 2023, **3**, 134-140.
13. J. Wang, Q. Niu, T. Wei, T. Li, T. Hu, J. Chen, X. Qin, Q. Yang and L. Yang, *Microchem. J.*, 2020, **157**, 104990.